Attributing long-term changes in airborne birch and grass pollen concentrations to climate change and vegetation dynamics

Verstraeten, W.W.; Bruffaerts, N.; Kouznetsov, R.; Weger, L. de; Sofiev, M.; Delcloo, A.W.

Atmospheric Environment 298 (2023) 119643

Contents lists available at ScienceDirect

Atmospheric Environment

journal homepage: www.elsevier.com/locate/atmosenv

Attributing long-term changes in airborne birch and grass pollen concentrations to climate change and vegetation dynamics

Willem W. Verstraeten [a,*], Nicolas Bruffaerts [b], Rostislav Kouznetsov [c], Letty de Weger [d], Mikhail Sofiev [c], Andy W. Delcloo [a]

[a] Royal Meteorological Institute of Belgium, Ukkel, Brussels, Belgium
[b] Sciensano, Brussels, Belgium
[c] Finnish Meteorological Institute, Helsinki, Finland
[d] Leiden University Medical Center, Leiden, the Netherlands

HIGHLIGHTS

- 38 years of spatially distributed modelled daily birch and grass pollen concentrations.
- Temporal trends on spatially distributed daily airborne birch and grass pollen and weather data from Theil-Sen slopes.
- Associations between daily pollen concentrations and meteorological variables from Kendall correlations.
- Attribution of long-term pollen concentration trends to changes in climate and/or vegetation dynamics.

GRAPHICAL ABSTRACT

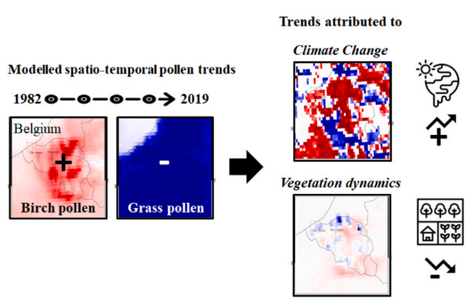

ARTICLE INFO

Keywords:
Aerobiology
Birch & grass pollen
Climate change
Chemistry transport model
Pollen source

ABSTRACT

Changes in climate and land-use may elicit an increased emission of allergenic pollen amounts in the air, causing a rise in respiratory allergies and affecting public health more than previously thought. Here we have used a well-established pollen transport model SILAM (System for Integrated modeLling of Atmospheric coMposition) for attributing the long-term changes in airborne pollen concentrations of birches and grasses to climate change and vegetation dynamics. The pollen transport model is applied for Belgium and is driven by ECMWF ERA5 meteorological data (European Centre for Medium-Range Weather Forecasts, fifth generation of ECMWF atmospheric reanalysis of the global climate). The dynamic vegetation components of the model are based on multi-decadal datasets for 1982–2019 on spatially distributed birch and grass pollen emission sources. For each model gridcell we have computed the change rate of the seasonal birch and grass pollen cycles based on daily pollen concentrations, and of the daily meteorological model input. Finally, the gridcell based association between trends in pollen and climate change are derived. Our findings show that during the period 1982–2019 a strong increase in birch pollen concentrations is associated with increasing radiation, decreasing precipitation and decreasing horizontal wind speed near the surface. A strong decrease of grass pollen concentrations over time is driven by a decreasing trend in grass pollen sources, and it is also associated with decreasing precipitation. The magnitude of the associations between meteorology and airborne birch pollen concentrations are almost twice the association

* Corresponding author.
E-mail addresses: Willem.Verstraeten@meteo.be (W.W. Verstraeten), Nicolas.Bruffaerts@sciensano.be (N. Bruffaerts), Rostislav.Kouznetsov@fmi.fi (R. Kouznetsov), L.A.de_Weger@lumc.nl (L. de Weger), Mikhail.Sofiev@fmi.fi (M. Sofiev), Andy.Delcloo@meteo.be (A.W. Delcloo).

https://doi.org/10.1016/j.atmosenv.2023.119643
Received 7 October 2022; Received in revised form 6 January 2023; Accepted 5 February 2023
Available online 8 February 2023

between meteorology and grass pollen, and the spatial variations are substantial even on the scales of small countries. The specific contribution of birch tree and pollen production dynamics to the concentrations of birch pollen in the air over time is highly associated with wind speed and precipitation. Introducing the inter-seasonal variation in birch pollen production during the period 1982–2019 intensifies the climate induced increase of airborne birch pollen concentrations with ~6%. In contrast, the grass pollen production dynamics resulted into ~10 times less grass pollen over the studied period compared to climate change effects.

1. Introduction

Airborne pollen is a substantial cause of respiratory allergies impairing public health, especially in combination with long-term exposure to other air pollutants (D'Amato et al., 2007). In Europe, more than 20% of the population suffers from pollinosis (WHO, 2003). In the northwestern countries such as Belgium, the Netherlands and Luxembourg (abbreviated as Benelux) the prevalence of allergic rhinitis is estimated to be 10–30% (To et al., 2012; Bauchau and Durham, 2004; Blomme et al., 2013). In Belgium, a highly industrialized and densely populated country with substantial air pollution (Verstraeten et al., 2018), at least ~10% of the people develop allergic rhinitis symptoms due to birch tree pollen and ~15% due to grass pollen (Blomme et al., 2013). In the future, even more people might be affected since climate change and land-use change elicit an increased amount of allergenic airborne pollen and prolonged pollen seasons (Anderegg et al., 2021; Beggs, 2021; Tong et al., 2022). The human influence on the climate system is clear-cut (IPCC, 2022), and the changes in climate, for instance the worldwide increased temperature of 1.2 ± 0.1 °C, have multiple impacts on the environment and public health (WMO, 2020).

The observed warming and the increasing temperature extremes might already contribute to longer pollen seasons, earlier start of the season and an increased pollen load for several allergenic pollen taxa in the northern hemisphere in general (Ziska et al., 2019) and more specific in North America (Anderegg et al., 2021; Zhang and Steiner, 2022). Additional carbon dioxide (CO_2) might increase the pollen amount, the seasonal intensity, and even the allergen concentration of the pollen. Consequently, it might aggravate the symptom severity (Ziska, 2021; Zhang and Steiner, 2022). Moreover, also other vegetation related changes can influence the production of aeroallergens, increase exposure, and may have consequences for public health (Ziska, 2021). For instance, changing vegetation height affects pollen dispersion in combination with changing wind patterns and speed. Climate induced changes in the composition of vegetation in favor of allergenic species may increase the impact on patients suffering from allergic diseases. Lack of proper vernalization can reduce floral initiation, but warmer spring temperatures may accelerate floral bud development and opening (Ziska, 2021). Other biotic (for instance plant diseases) and abiotic (wind, water, mineral stress, air pollution) environmental interactions may change the impact of pollen exposure in favor or disfavor of patients suffering from respiratory allergies (Ziska, 2021).

For Europe, studies have shown significant increasing airborne pollen concentration trends in relation to the changing climate and shifts in the timing of the pollen seasons in some northern parts (Bruffaerts et al., 2018; Hoebeke et al., 2018; Lind et al., 2016) and southern parts of Europe (Damialis et al., 2007; Galán et al., 2016; Velasco-Jiménez et al., 2020). More specific, for the Benelux, airborne pollen of most tree species showed an overall trend towards an increase in peak values and in the Seasonal Pollen Integral (SPIn) with an overall trend towards an earlier start and end of the pollen season (de Weger et al., 2021). For birch pollen, a trend towards a decrease in pollen season length was observed. In the Benelux, herbaceous species showed a decreasing trend in the SPIn and lower peak values. The grass pollen season shifted towards earlier starts and longer seasons (de Weger et al., 2021).

Attributing the long-term changes in the emissions of birch and grass pollen to climate change and vegetation dynamics requires a modelling approach. Only well-established pollen transport models are capable of simulating the pollen concentrations near the surface taking into account all the processes involved such as pollen release, airborne transport and surface deposition. The most advanced model scenario for airborne pollen concentrations includes a dynamic vegetation component that reflects the variability of intra-seasonal pollen production and emissions on top of the varying meteorological conditions. For quantifying the exclusive impact of climate change on pollen emission we use a reference or basic scenario model run with a fixed or time invariant vegetation component in a bottom-up pollen emission approach. By subtracting these two model scenarios (the advanced and reference run), the impact of the vegetation component on the amount of pollen in the air can be quantified. Here, we apply multi-decadal datasets on birch and grass pollen emission sources as the dynamic vegetation components into the pollen transport model SILAM (System for Integrated modeLling of Atmospheric coMposition, http://silam.fmi.fi) (Sofiev et al., 2013, 2015). SILAM is applied for Belgium at a 0.1° × 0.1° grid using meteorological data from the ECMWF (European Centre for Medium-Range Weather Forecasts) for the period 1982–2019, covering almost four decades (ECMWF, 2020). In Belgium, we have a continuous long-term dataset of atmospheric concentrations of various pollen species at Brussels (Elsene, 50.825 N/4.383 E) since 1982, and at De Haan at the coast side (51.274 N/3.022 E) since 1984. SILAM is a well-established model (Vélez-Pereira et al., 2022) and has been thoroughly evaluated for Belgium based on historical pollen observations from the Belgian aerobiological surveillance network (Verstraeten et al., 2019; Delcloo et al., 2020; 2021; Verstraeten et al., 2021; 2022). The multi-decadal datasets on birch and grass pollen emission sources has been developed by merging spaceborne vegetation index data with areal vegetation maps using the Random Forest statistical methodology as described in Verstraeten et al. (2022). In order to explore the spatial behavior of the modelled birch and grass pollen concentrations over time for the different scenarios, we compute the change rate in the seasonal birch and pollen cycles based on daily pollen concentrations. This is also done for meteorological variables. Finally, the association between daily pollen trends and trends in meteorology are derived for each gridcell of the model (Bruffaerts et al., 2018).

In short, the objective of this study is attributing the long-term changes in airborne birch and grass pollen concentrations to climate change and vegetation dynamics. A multi-decadal dataset (1982–2019) on birch and grass pollen emission sources is ingested into the pollen transport model SILAM to retrieve airborne pollen concentrations. We then compute the temporal change rate of the modelled airborne pollen concentrations for each day of the 1982–2019 birch and grass pollen seasons, as well as for the corresponding meteorological variables to estimate the association with trends in pollen. By comparing these trends with trends of airborne pollen concentrations obtained with SILAM based on only one fixed (time-invariant) birch and grass pollen emission source, we then can attribute the contribution of climate change or effects of vegetation dynamics to the retrieved trends in airborne pollen concentrations.

2. Methodology

2.1. Pollen transport model SILAM

Pollen grains are biogenic aerosols which are much larger than conventional (anthropogenic and non-biogenic) atmospheric aerosols.

The main processes involved in aerosol modelling and thus pollen transport include wind advection, mixing due to turbulence, and dry and wet deposition. These processes are integrated into SILAM (Sofiev et al., 2006; Kouznetsov and Sofiev, 2012; Sofiev et al., 2015). SILAM is a large-scale dispersion model developed for atmospheric composition and air quality and it includes both Lagrangian and Eulerian advection-diffusion formulations. Here, the Eulerian or box mode is used with a basic horizontal grid cell resolution of 0.1 × 0.1° and a vertical resolution consisting of an uneven distribution of nine layers (thickness of layers from surface to the free troposphere is 25, 50, 100, 200, 400, 750, 1200, 2000, and 2000 m).

The procedure of the pollen emission is different for birch and grass pollen. The start and end of the flowering season of birches, i.e. the period of the pollen emissions, in SILAM is based on the thermal time flowering model (Sofiev et al., 2006) and is parameterized using temperature sum thresholds (Linkosalo et al., 2010; Sofiev et al., 2013). The timing of birch flowering is assumed to be mostly driven by accumulated ambient temperature. The cumulative fraction of pollen emitted from the start to the end of the pollen season is assumed piecewise linear and proportional to the temperature sum during the main flowering season. The grass pollen emission computations in SILAM do not rely on the temperature sum. The emitted amounts of airborne grass pollen grains are computed by the multiplication of the grass pollen source map for each gridcell with the emission rate determined by the prescribed shape of the grass flowering intensity stretched from the season's start to the season's end (see also Fig. 3 in Sofiev, 2017). This function is the average shape of the seasonal distribution of the seasonal pollen grains production during the grass flowering period. The onset and offset of this period follow a location-dependent prescribed calendar expressed in Julian days.

Short-term meteorological conditions affect the amount of airborne birch and grass pollen depending on the specific aerodynamic properties. Precipitation and humidity inhibit the emission of pollen from vegetation, while high wind speed favors the pollen emission. ECMWF (European Centre for Medium-Range Weather Forecasts) ERA5 (fifth generation of ECMWF atmospheric reanalysis of the global climate) reanalysis meteorological datasets (gridcell of 0.25° × 0.25°) (ECMWF) are used to drive the transport, emission and deposition of airborne pollen in SILAM. In Belgium, the general birch pollen season ranges from March to June (largest amounts in April), and the grass season from May to August (largest amounts in June).

Modelling the airborne birch and grass pollen concentrations near the surface in SILAM is based on a bottom-up approach using inventories of birch and grass pollen sources. Hence, maps with the areal fractions of birches and grasses are crucial underlying datasets. At the European scale, birch and grass pollen emissions maps were first compiled and refined by Sofiev et al. (2006) and Sofiev et al. (2013), respectively. Recently, we have merged the birch tree fraction map on the European scale with forest inventory data of birch trees on the scale of Belgium (see for details: Verstraeten et al., 2019) to improve the local birch pollen emissions. We also have updated the European MACCIII grassland map using the Copernicus Land Monitoring Service (CLMS) (2015) land-use maps on a 100m spatial resolution (Copernicus, Langanke, 2017) scaled to the 0.05° × 0.05° gridcell. The updated map is the maximum value of the combination of the European grassland data from CLMS and the MACCIII map (see for details: Verstraeten et al., 2021). In order to introduce pollen emission maps for each season from 1982 to 2019, multi-decadal datasets on birch and grass pollen emission sources were developed by merging spaceborne NDVI data (Normalized Difference Vegetation Index, Tucker, 1979) with the above mentioned birch tree fraction and grass pollen emission maps using the Random Forest statistical methodology as described in Verstraeten et al. (2022). The compiled NDVI dataset is a combination of the GIMMS NDVI3g (Pinzon and Tucker, 2014) data covering 1982–2015 and the METOP AVHRR NDVI (ENDVI10, ENDVI10, 2021) data covering the period 2009–2019. Illustrations of areal birch fraction and grass emission maps are given in Fig. 1.

2.2. Attribution of change rate

In order to attribute changes in airborne pollen concentrations over time to climate change or to vegetation dynamics, we compute trends and associations between trends in meteorological variables and pollen concentrations obtained from SILAM. We apply the methodology described in Bruffaerts et al. (2018) based on Makra et al. (2011) and also used in de Weger et al. (2021). The first part determines the change rate. The procedure to derive temporal trends (the change rate) of pollen concentrations begins with the time series of daily pollen concentrations of birches and grasses for each gridcell of Belgium as modelled by SILAM (i) covering the period 1982–2019 (38 years). A typical example of such a time series is shown in Fig. 2(a) for airborne birch pollen concentrations extracted for the gridcell of Brussels. In the next step (ii), we

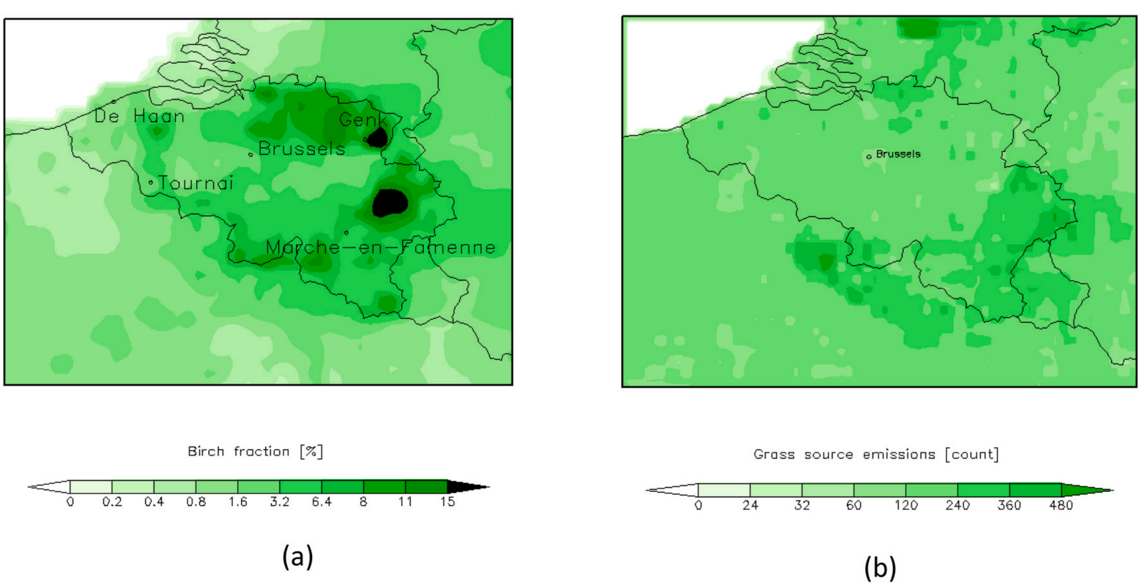

Fig. 1. (a) Spatial distribution of areal birch tree fractions (percentage) in Belgium based on forest inventory data (see Verstraeten et al., 2019 for details, produced with Grads). (b) Similar, but for grasses expressed as the amount of emitted pollen (counts) (Verstraeten et al., 2021).

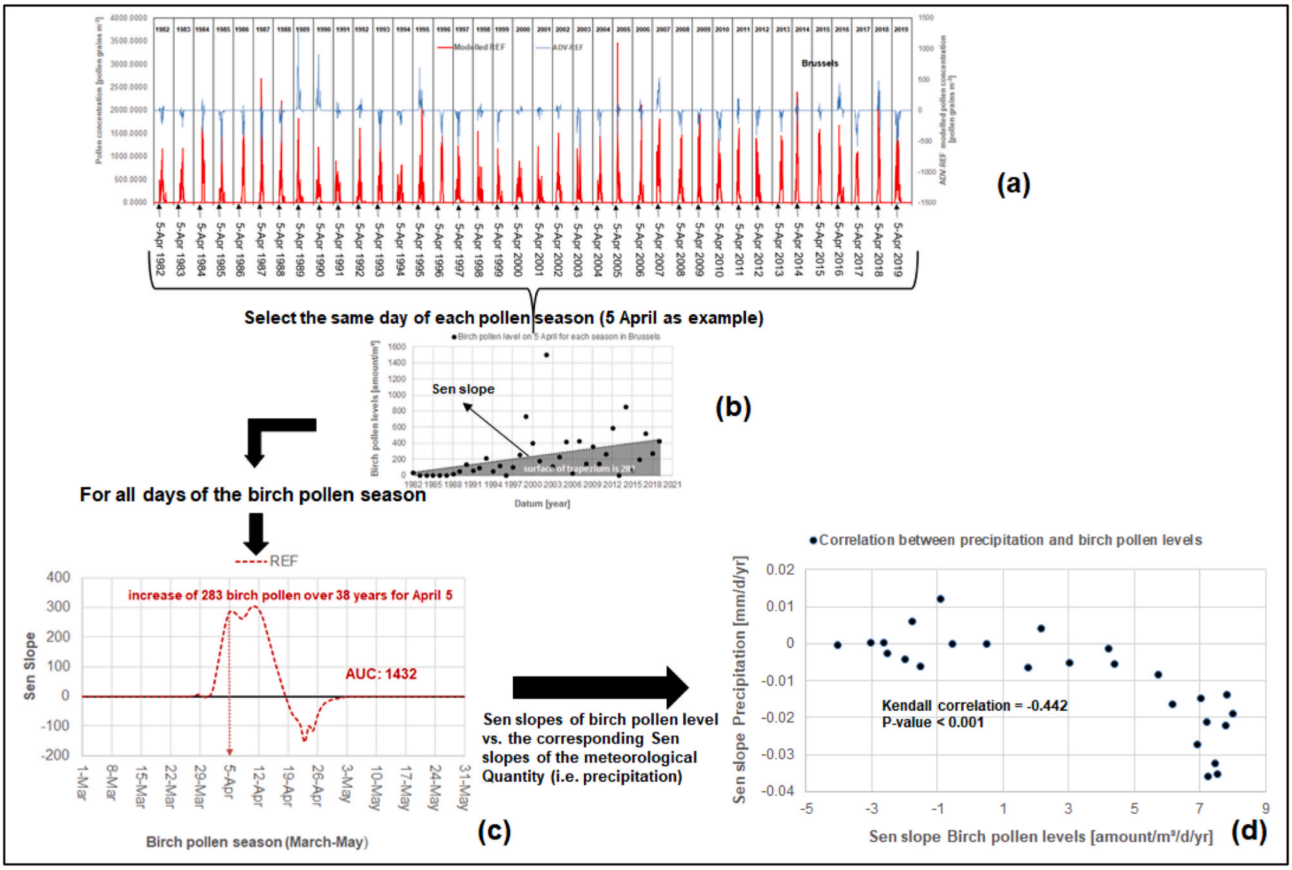

Fig. 2. Computation procedure of associating the change rate of pollen concentrations with meteorological variables. (a) SILAM modelled airborne birch pollen concentration time series (in red) for one location (gridcell with Brussels as example) for the period 1982–2019 (example Reference or REF scenario). (b) Selection of the same day of every pollen season (example 5 April) from 1982 to 2019. Calculating the Theil-Sen slope from the regression of 38 values of that specific day. Compute the surface of the trapezium (in grey) determined by the regression function (c). Repeating this for all days of the pollen season. Smoothing the Theil-Sen slope values determined from the trapezoidal shape. AUC is the sum of the area determined by the curve. (d) Comparison of the birch pollen concentration Theil-Sen slopes for every day of the pollen season with the corresponding Theil-Sen slopes of the meteorological variables (example precipitation). Computation of the Kendall correlation from these Theil-Sen slope pairs over the pollen season.

compute the Theil-Sen slope values for each day of the birch (and also grass) pollen season for the period 1982–2019. The Theil-Sen slope is a method for robustly fitting a line to sample points in the plane (simple linear regression) by choosing the median of the slopes of all lines through pairs of points (Theil, 1950; Sen, 1968). It is based on non-parametric statistics and the estimator is insensitive to outliers. For the birch season we start at March 1st, and we construct a time series of all March 1st values from 1982 to 2019 (38 values). On these 38 values the Theil-Sen slope is derived, as illustrated in Fig. 2(b). We compute the area under the trapezium (trapezoidal method) determined by the linear regression using the Theil-Sen slope (representing the 38-year period total increase/decrease of pollen concentrations), only if the slope is significantly different from zero ($P < 0.05$, Mann-Kendall non-parametric procedure). The numerical value of the area under the trapezium is then plotted for March 1st. This is repeated for all the days of the birch season (March 1st – July 1st: 123 days) and we obtain the (red) curve in Fig. 2(c) after applying the LOcally Estimated Scatterplot Smoothing (LOESS) method (García-Mozo et al., 2014), setting the span to 0.1. Finally, we compute the Area Under the Curve, by summing all positive and negative values for all 123 days (iii). We obtain an AUC of 1432 in Fig. 2(c), which is positive (also considering the negative values during late April in Fig. 2(c)) indicating a strong increase in the amount of birch pollen in the air during the period 1982–2019 for the gridcell of Brussels. The same procedure is also applied to compute the AUC for the meteorological variables such as the daily mean, maximum and minimum air temperatures, the mean, maximum and minimum dew point temperatures, daily radiation, daily precipitation, horizontal wind components (North and East component) near the surface (10m) for the period 1982–2019 for each day of the pollen season and for each model gridcell.

In the second part, the association of pollen and climatic trends are estimated using the Kendall tau correlation on the pairs of the Theil-Sen slopes representing the pollen and the climatic trend for the same day of the pollen season. This means that the Theil-Sen slope for each day of the pollen season (derived in Fig. 2(b)) for birch pollen is paired with the Theil-Sen slope computed for a meteorological variable (precipitation in the example of Fig. 2) of the corresponding day. Hence, we obtain 123 pairs of Theil-Sen slope values (precipitation vs birch pollen) as illustrated in Fig. 2 (d) (only non-zero values are shown) used for the computations of the Kendall tau correlation. This procedure (Fig. 2) is repeated for the grass pollen and the corresponding meteorological variables also spanning 123 days (grass pollen season from May 1st until August 31st).

Basically, for each pollen type we have three kinds of time series of daily airborne pollen concentrations for each model gridcell: (i) the reference model run (REF) where the vegetation component is time invariant (fixed pollen emission for 38 seasons), (ii) the advanced model run (ADV) including vegetation dynamics (38 seasons with varying pollen emissions), and (iii) the difference between the advanced (ADV) and reference (REF) model run (ADV-REF) to isolate the sole effect of the changing pollen emissions over time. For each of the three kinds of pollen concentration time series, the Kendall tau associations are computed for each meteorological variable (mean, maximum and minimum air temperatures; mean, maximum and minimum dew point temperatures; radiation, precipitation, horizontal wind components near the surface). Finally, the Kendall tau correlations are mapped for each model gridcell. Fig. 9 in section 3.3 illustrates the applied procedure of computing Theil-Sen slopes, AUC values and Kendall tau correlations for birch and grass pollen levels and precipitation, radiation and wind for the three SILAM scenarios (REF, ADV, ADV-REF) as an example for the gridcell of Brussels for 1982–2019. This methodology has the advantage that the overall trend reflected by the AUC compared to trends directly computed on the SPIn for instance keeps its sensitivity for day-to-day change due to the difference in the integration time (daily change rate versus fixes seasonal length). Averaging the values of daily slopes of linear trends over the pollination seasons (this is essential what AUC does) gives rates of change of the total annual pollen counts even when overall trends are not significant at the 10% level (Makra et al., 2011). Moreover, using day-to-day change associations between trends of different variables can be computed.

3. Results and discussions

3.1. Association between daily birch pollen concentrations and meteorological variables

As an indicator for overall trend to explore the behavior of the birch pollen over time, the Area Under the Curve (AUC) was calculated as illustrated into Fig. 2. A substantial increase of airborne birch pollen amounts over the period 1982–2019 is found for both the SILAM reference scenario (focusing on the impact of climate change on birch pollen concentrations only) as well as for the advanced scenario (combining vegetation dynamics and climate change) as shown in Fig. 3a and b. Both scenarios have large positive AUC values, indicating that the birch pollen increase in the air is mainly climate change driven. The spatially distributed AUC values for the birch pollen concentrations time series that are based on the difference between the advanced and reference scenario run of SILAM are mainly negative for the northern part of Belgium (Fig. 3(c)).

The spatially averaged AUC value for the reference model scenario is ~1040. This is somewhat smaller than for the advanced scenario (~1075) (Fig. 3). The contribution of the vegetation dynamics counts for a positive $AUC_{ADV\text{-}REF}$ value (~66), which is ~6% of AUC_{REF}. This suggests that introducing dynamic birch tree fraction maps for the period 1982–2019 may intensify the climate change induced increase of the amount of birch pollen in the air. However, there are regional differences where the $AUC_{ADV\text{-}REF}$ values are negative (in blue), mainly occur on locations with increased amount of birch trees compared to the reference map (Verstraeten et al., 2019).

The spatial distributions of the AUC values for daily rainfall, mean air temperature, mean dew point temperature, radiation, and the horizontal wind velocity components from ERA5 during the birch pollen season (March–June), used as input in the SILAM model, for the period 1982–2019 are shown in Fig. 4. A substantial decrease in the AUC values for precipitation and the horizontal wind speed are found while radiation, the mean and dew point temperatures show large increases (Fig. 4). Less precipitation and higher temperatures are in favor of higher airborne birch pollen amounts.

Association of pollen and meteorological trends are estimated using the Kendall tau correlation of pairs of Theil-Sen slopes. For every day of the birch pollen season, the Theil-Sen slope of the pollen concentrations derived from SILAM is compared with the Theil-Sen slope of the specific meteorological variables (see also Fig. 2). This is done for all the meteorological variables. We apply this procedure for the reference and advanced scenario, and for the time series derived as the difference between the two scenarios (runs from March 1^{st} till July 1^{st}). The spatial distributions of the Kendall tau correlations between each pollen scenario and precipitation, radiation, and the horizontal wind speed components are illustrated in Fig. 5. From the reference and advanced SILAM scenario a substantial increase of the amount of birch pollen in the air is associated with a decrease (in blue) in rainfall, WU (i.e. eastward component of horizontal wind speed) and to a lesser extend WV (i.e. northward component of horizontal wind speed), and an increase (in red) in radiation (but not for central Belgium).

In order to isolate the impact of the introduced decadal birch pollen emission maps, i.e. the dynamic vegetation component, the difference scenario (ADV-REF) is compared with meteorological variables. For some (mainly but not exclusively northern) parts of Belgium, substantial decreases in the amount of airborne birch pollen induced by the dynamic vegetation component (covering both natural as anthropogenic changes in land-use) are associated with a decrease in rainfall and of the WU (eastward) wind component, and an increase in radiation. Most model gridcells do not contain statistical significant correlations (P-value >0.05) for all the other meteorological variables (minimum, mean

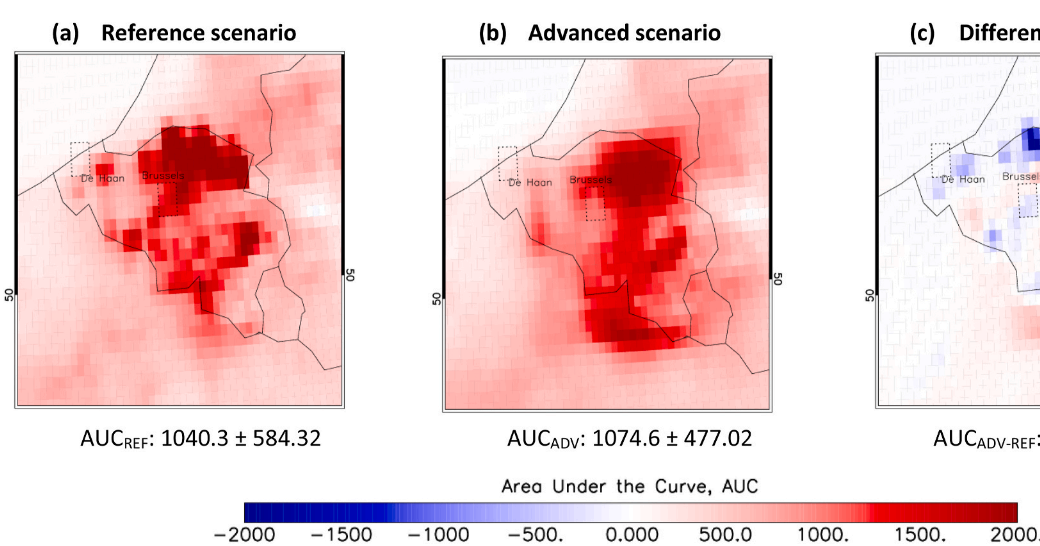

Fig. 3. (a) Spatial distribution of the Area Under the Curve (AUC) values of **airborne birch pollen concentrations** for Belgium based on the reference scenario of SILAM for the period 1982–2019. (b) Same as for (a) but using the advanced scenario of SILAM. (c) Same as for (a), but the AUC is computed from the time series of the difference between the advanced (ADV) and reference (REF) SILAM. The locations with the longest time series of observed pollen concentration are indicated as rectangles (Brussels at 50.825 N/4.383 E; De Haan at 51.274 N/3.022 E). The spatially averaged AUC values (±st dev) for Belgium are also provided.

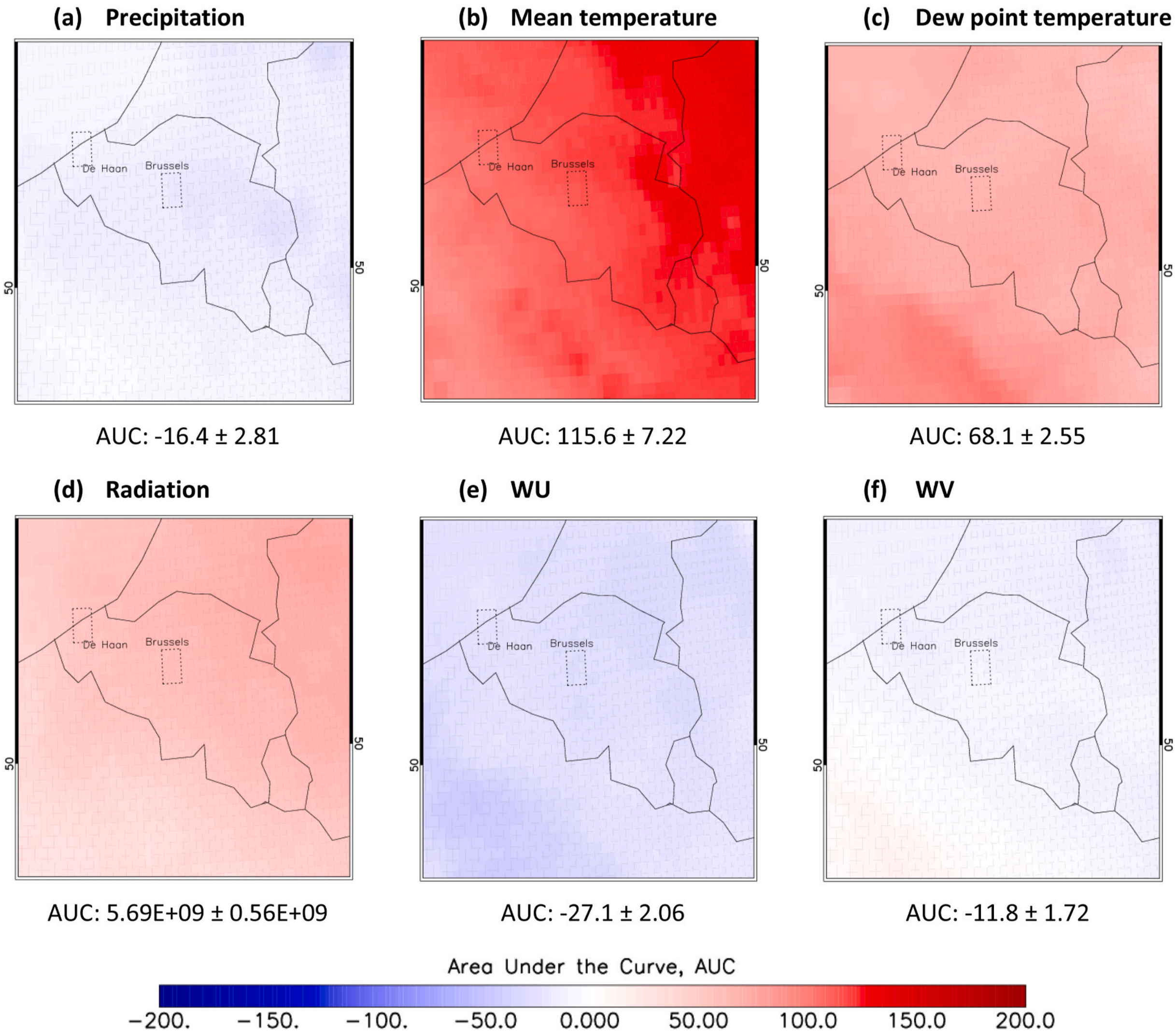

Fig. 4. Spatial distribution of the Area Under the Curve (AUC) of a selection of **ERA5 meteorology** during the **birch pollen season** (March–June) for the period 1982–2019 in Belgium. (a) Daily precipitation, (b) mean air temperature, (c) mean dew point temperature, (d) radiation, (e) the horizontal wind speed WU, and WV (f). Radiation is scaled with 1E-08. The spatially averaged AUC values (±stdev) of each map are also provided.

and max air temperatures and minimum, mean and max dew point temperatures) and are not shown. The spatially averaged Kendall tau correlations for the maps between birch pollen concentrations of the REF and ADV model scenarios and used meteorological variables are positive for radiation and negative for precipitation and wind speed. The birch pollen difference scenario shows opposite correlations with the respective meteorological variables. For computing the spatially averaged correlation value only correlation values are considered which were statistically significant different from zero (P-value <0.05). Regionally, the sign of the correlations can be reversed.

3.2. Association between daily grass pollen concentrations and meteorological variables

For evaluating the change of daily grass pollen concentrations over time and the association with meteorological variables the same analysis as for the birch pollen (section 3.1) was carried out. Fig. 6 shows the small increase in the amount of grass pollen over 1982–2019 due to climate change only (Fig. 6(a)), which is more than ten times lower for the advanced scenario (AUC_{REF} = ~55 versus AUC_{ADV} = ~-531) (Fig. 6(b)). Introducing dynamic grass pollen emission maps leads to much smaller amounts of airborne grass pollen over time (Fig. 6(c)) as compared with time invariant grass maps ($AUC_{ADV\text{-}REF}$ = ~-507 or half the AUC_{ADV} and almost ten times smaller than the AUC_{REF}). The values of the AUC's for birch and grass pollen are substantially different in sign and the absolute values, since also the total amount of emitted pollen is different. Consider that the average grass SPIn for Brussels is only ~45% of the birch SPIn, but for the coast side it is rather similar. In the birch tree rich areas of Belgium, the grass SPIn is only 20% of the birch SPIn.

Similar to the birch pollen, the spatial distribution of the AUC values for some meteorological variables during the grass pollen season (May–August) for the period 1982–2019 are shown in Fig. 7.

Decreases in precipitation in large parts of Belgium are observed, but less pronounced in the south. The other meteorological variables increase over time, especially the mean temperature. The horizontal wind speeds near the surface shows only some slightly higher values over time. Generally, the absolute AUC values of the meteorological variables for the grass season are smaller than those of the birch season (except for WV) notwithstanding the fact that the grass pollen season is in general somewhat longer.

The spatial distributions of the Kendall tau correlations between each grass pollen scenario and precipitation, radiation, and the horizontal wind speed components for May–August are given in Fig. 8.

The slight increases in the amount of grass pollen over time derived from the REF model run are associated with decreases in rainfall over large parts of Belgium and in WU (i.e. eastward component of horizontal

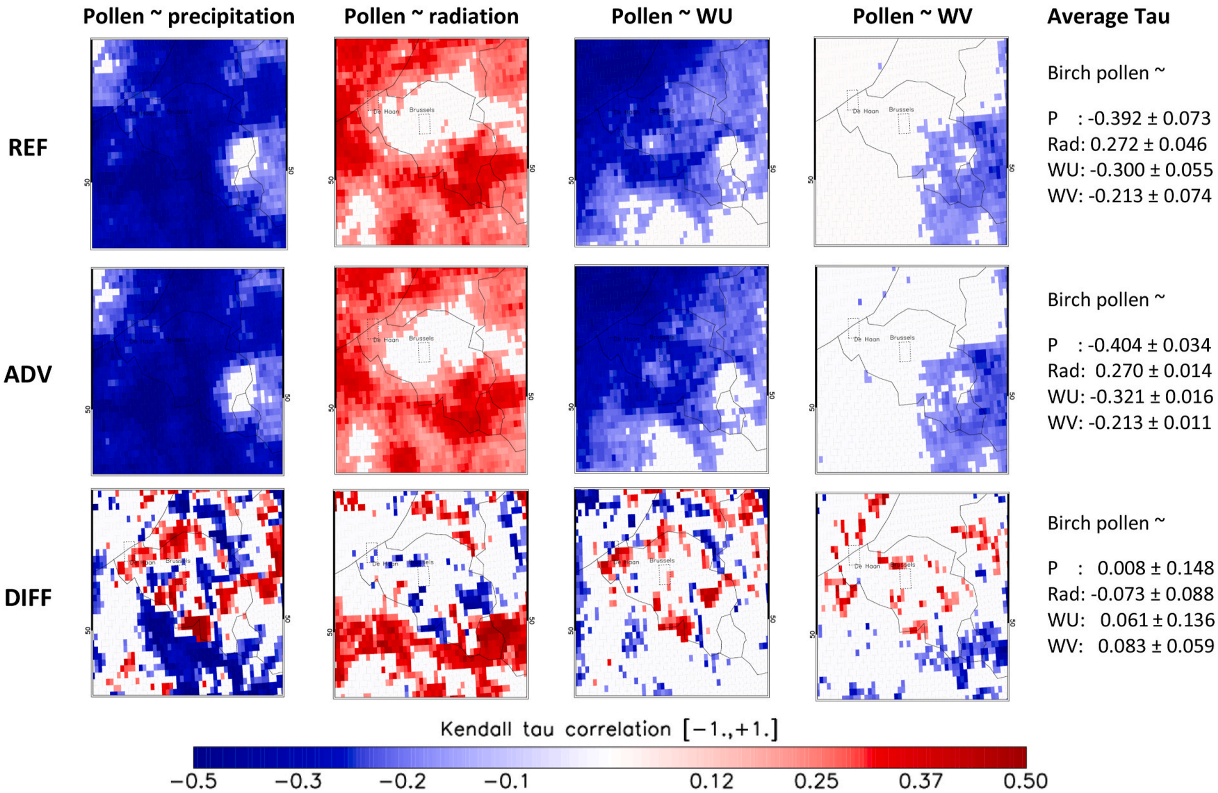

Fig. 5. Spatial distribution of the Kendall tau correlation for on one hand the **birch pollen concentrations** derived from the reference and advanced SILAM scenarios, and from the difference time series, and on the other hand the **meteorological variables** precipitation, radiation and horizontal wind speed components. Only significant correlations (P-value <0.05) are shown, based on Mann-Kendall non-parametric procedure. The spatially averaged correlation (tau) and the stdev for each map are also given (right column).

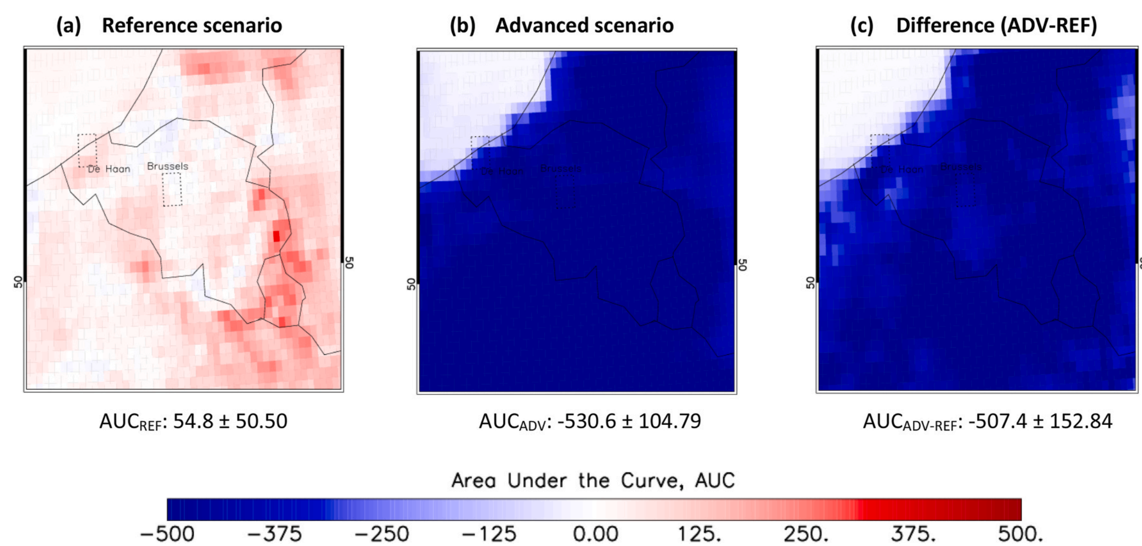

Fig. 6. (a) Spatial distribution of the Area Under the Curve (AUC) values of **airborne grass pollen concentrations** for Belgium based on the reference scenario of SILAM for the period 1982–2019 (left panel). (b) Same as for (a) but using the advanced scenario of SILAM (middle panel). (c) Same as for (a), but the AUC is computed from the time series of the difference between the advanced (ADV) and reference (REF) SILAM (right panel). The average AUC values (±stdev) of each map are also provided.

wind speed near the surface), a slight increase in WV (northward wind component) and a stronger rise in radiation (Fig. 8, panels of the first row). The introduction of dynamic grass maps (covering both natural and anthropogenic changes in land-use) decreases the amount of grass pollen in the air over time (Fig. 6(b,c)). The obtained reduction is mainly positively associated with changes in precipitation (Fig. 8, lower left panel). This means that decreases in precipitation (and to a lesser extend horizontal wind speed near the surface) over time corresponds to decreases in grass pollen concentrations induced by the dynamic vegetation maps which alterations are partly human-induced. For radiation, a mixed situation is obtained when the contribution of the grass pollen emission source dynamics is considered. Most parts of Belgium remain

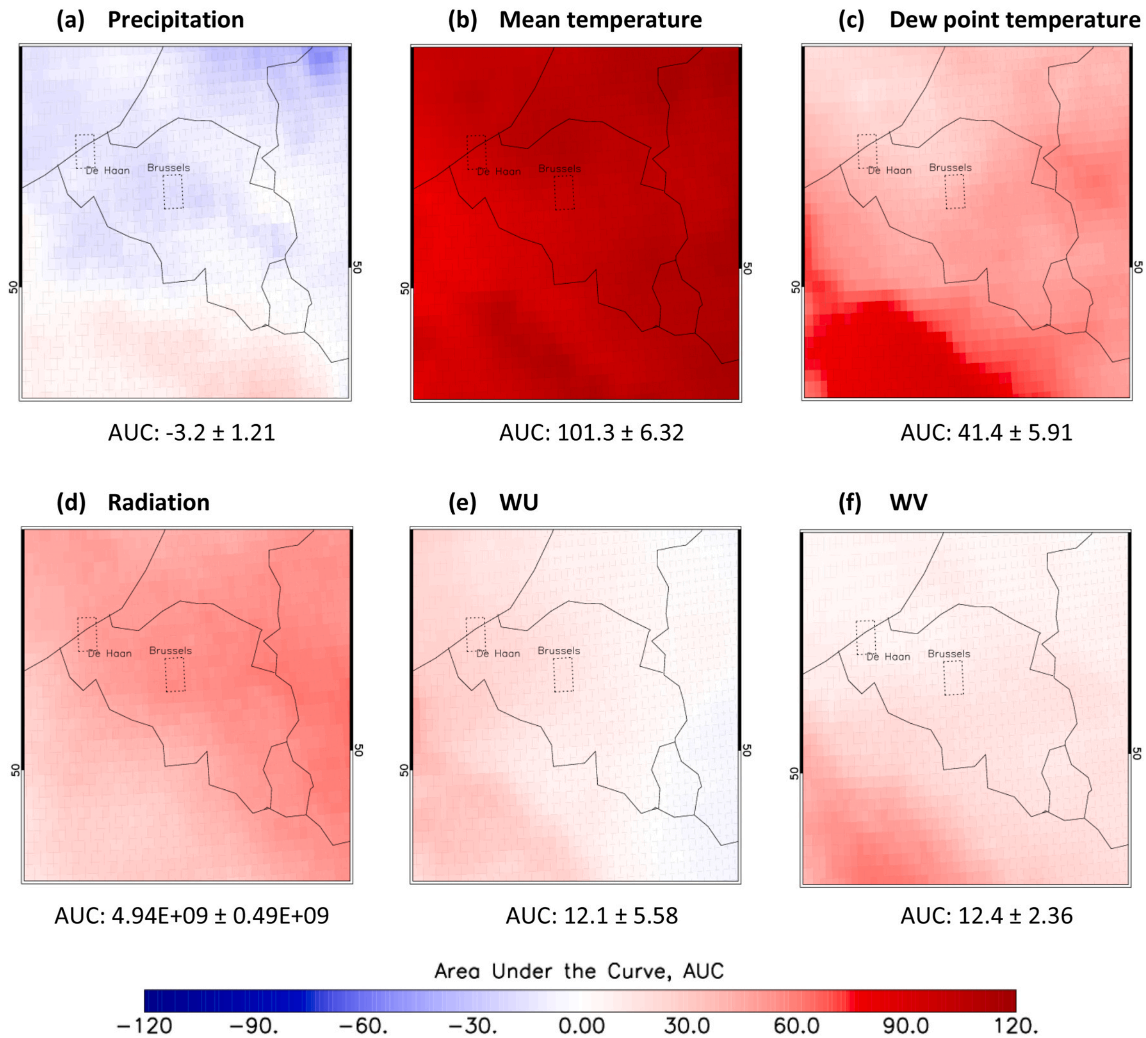

Fig. 7. Spatial distribution of the Area Under the Curve (AUC) of a selection of **ERA5 meteorological variables** during the **grass pollen season** (May–August) for the period 1982–2019 in Belgium. (a) Daily precipitation, (b) mean air temperature, (c) mean dew point temperature, (d) radiation, (e) the horizontal wind speed WU, and WV (f). For representation, the AUC of precipitation is scaled with 3, and for radiation with 10^{-8}. The average AUC values (±stdev) of each map are also provided.

white (i.e. no significant change, P-value ≥0.05). The grass dynamic component has slightly negative associations for radiation and positive for the wind components on the amount of pollen. In general, the grass pollen associations with climate change are smaller than the birch pollen associations (see ratios of the provided spatially averaged correlation values in Figs. 5 and 8).

3.3. Further interpretation

In order to illustrate the interpretation of the Kendall tau correlations in Figs. 5 and 8, time series of the Theil-Sen slopes of birch and grass pollen concentrations derived from the SILAM scenarios and the corresponding Theil-Sen slopes of the meteorological variables (see Figs. 5 and 8) are extracted for the Brussels gridcell (Fig. 9). For example, the ADV-REF birch pollen concentration scenario (Fig. 9, first row) shows negative Theil-Sen slopes (black dashed) in the first half of April. In the same period the Theil-Sen slopes of the precipitation are also negative. This results into a positive Kendall tau correlation (Fig. 9, third row, green). Overall, for the REF and ADV scenarios (positive Theil-Sen slopes in first half of April), the correlation with precipitation is negative (negative Theil-Sen slopes).

The lower amounts of precipitation during the peak of the birch pollen season (less wet deposition of pollen to the ground) in combination with more radiation (clearer skies, more plant activity) decreasing wind speeds (in favor of emissions that have a local character, if the wind speed is not too low), might explain the higher pollen concentrations over time. For grass pollen the association is more complex. Overall, the AUC_{REF} value for grass pollen is positive while the AUC_{ADV} and $AUC_{ADV\text{-}REF}$ values are negative, as well as the AUC of the precipitation. Examining the Theil-Sen slopes of the pollen concentrations from the advanced model scenario and the precipitation, however, shows that the slopes tend to be contra-acting. The Theil-Sen slopes for the pollen from the ADV and ADV-REF model scenarios are negative while the slopes for precipitation show more variation. Early and late June, the slopes for precipitation are negative, while in mid-June and August the slopes are generally positive. Overall, combining all pairwise Theil-Sen slopes returns positive associations for the ADV and ADV-REF model runs as shown in the third panel of Fig. 9.

The changing climate has been affecting the concentrations of allergenic pollen. For the Benelux, airborne pollen of most tree species showed an overall increasing trend in peak values and in the SPIn (de Weger et al., 2021), which corroborates our findings of the large positive AUC values for birch pollen concentrations. Although, the warming is reported to contribute to increased pollen load for several allergenic pollen taxa in the northern hemisphere (Ziska et al., 2019), our analysis indicates that during the birch pollen season the increased pollen

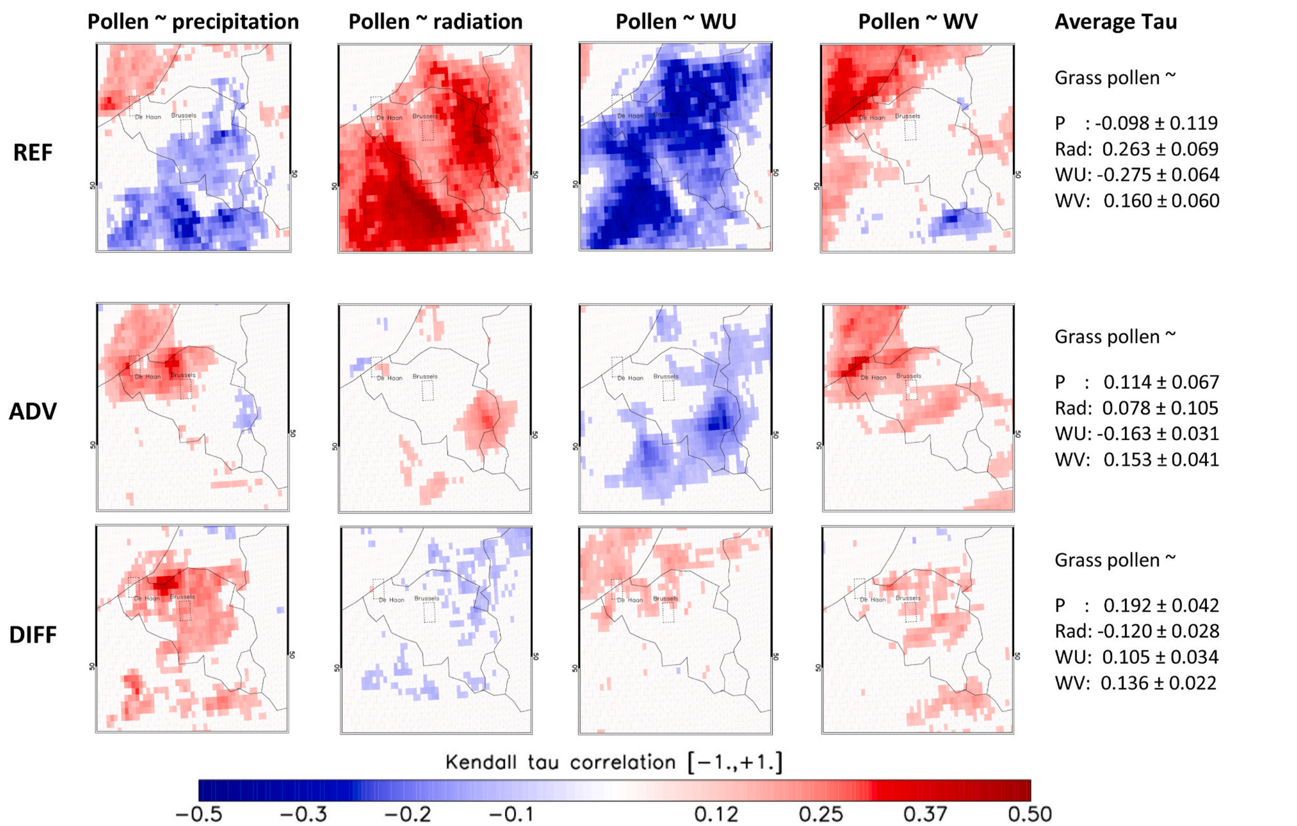

Fig. 8. Spatial distribution of the Kendall tau correlation for on one hand the **grass pollen concentrations** derived from the reference and advanced SILAM scenarios, and from the difference time series, and on the other hand the **meteorological variables** precipitation, radiation and horizontal wind speed components. Only significant correlations (P-value <0.05) are shown. The spatially averaged correlation (tau) and the stdev for the maps are also given (right columns).

concentrations over time (1982–2019) are strongly associated with decreasing precipitation, lower wind speed, and higher radiation (not for central Belgium). The association with rising temperature (especially maximum temperature) is substantial for the southern half of Belgium, but not for the northern part in Flanders. This is in line with the analysis of the observed birch pollen concentrations in the Benelux (de Weger et al., 2021) and for SPIn in the US (Zhang and Steiner, 2022). As shown in Fig. 10 (left panel), substantial increases of birch pollen emissions sources have been observed for Belgium. Locally some significant decreases pop-up. For the grass pollen concentrations, a decline in the pollen amounts was also reported for the Benelux between 1982 and 2020 (de Weger et al., 2021), which corresponds to the decreasing trend observed at Brussels for the period 1982–2015 (Bruffaerts et al., 2018). For the US, future changes in temperature and precipitation affect the grass pollen negatively (Zhang and Steiner, 2022), and changes in land-use show a mix of decreasing and increasing effects. This corroborates with our results from the advanced model run based on the grass pollen emission sources that show a substantial decreasing trend (Fig. 10, right panel).

In Verstraeten et al. (2022), an AUC_{OBS} value of is ~790 was obtained based on the observation of Brussels from the Belgian aerobiological surveillance network (Hirst, 1952; Hoebeke et al., 2018) for the birch pollen season from 1982 to 2019. The AUC_{REF} of the SILAM reference scenario for Brussels is ~1430 while introducing the vegetation dynamics for the birch pollen emission maps results into a AUC_{ADV} value of ~1050 which is closer to the AUC_{OBS} (Verstraeten et al., 2022). Since the advanced SILAM run is closer to the observations, it might demonstrate the important impact of birch vegetation dynamics on the pollen concentrations in a changing climate. Also in Ireland, airborne birch pollen concentrations have risen over the last 40 years. Though, this was mainly attributed to increases in the fraction of birch trees in forest areas as well as ornamental use (Maya-Manzano et al., 2021). Increasing urbanization might also affect the rising allergenic pollen concentrations due to increased CO_2 (Ziello et al., 2012; Zhang and Steiner, 2022), or to the increased ornamental use of allergenic tree species (Aerts et al., 2021) combined with urban heat island effects (Charalampopoulos et al., 2021; Tong et al., 2022). A substantial decrease in birch pollen emission sources over the urban region of Brussels in the SILAM model (~−8% per decade, Fig. 10) suggests a large impact of climate on the birch pollen concentrations. We also must consider whether the European vegetation already started accommodating to the higher temperatures by decreasing the thermal sensitivity (Fu et al., 2015).

The AUC_{OBS} for the grass pollen season from 1982 to 2019 for Brussels is ~ -245. The AUC_{REF} of the SILAM reference scenario is ~2 while introducing grass pollen emission dynamics resulted into a AUC_{ADV} value of ~ -490, reflecting the substantial decrease in grass pollen sources in the urban region of Brussels (−6.5% per decade, Fig. 10). The AUC_{ADV} value is closer to the magnitude and sign of AUC_{OBS}. At the coast side, we observe positive associations between the grass pollen decrease over time and all the considered meteorological variables except for the eastward horizontal wind component. For Brussels, most associations of pollen concentrations and meteorological variables are not significant. Only the northward wind component and precipitation show significant positive associations with the (decreasing) trend in grass pollen concentrations, and there is a negative association with the minimum dew point temperature. On average, negative associations between grass pollen concentrations and minimum, maximum and mean temperatures occur, as well as for the minimum dew point temperature and the eastward wind component. The other variables (mean dew point temperature, northward wind component, precipitation and radiation) are positively associated.

In this analysis we focused on the data pairs of pollen and meteorological variables, where we have compared the data for each day of

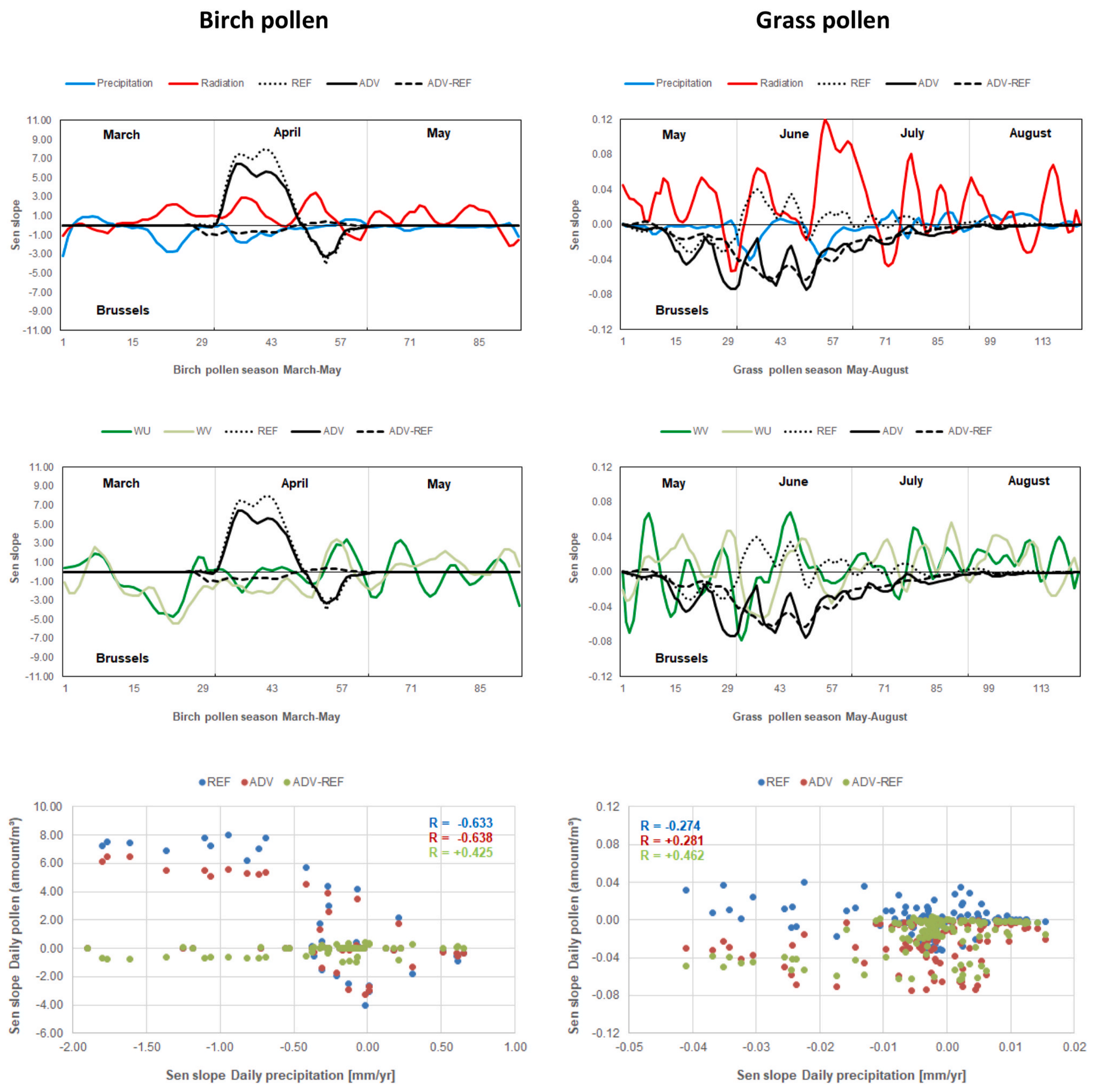

Fig. 9. Rate of change in the seasonal cycles of birch (left, March–June) and grass (right, May–August) pollen concentrations between 1982 and 2019 for the three SILAM scenarios (REF, ADV, ADV-REF) based on the Theil-Sen slope for every day of the season. The corresponding Theil-Sen slopes are also shown for radiation (red), precipitation (blue) (first row), and for the horizontal wind components (light and dark green, second row). Scatter plot with the Kendall tau correlation derived from pairs of the pollen Theil-Sen slopes and precipitation (third row). For graphical representation, scaling is applied on the Theil-Sen slopes of precipitation, wind components (factor of 50), radiation (2.5×10^{-6}) for the birch pollen season, and for the grass pollen season on radiation (10^{-8}) and on the pollen (10^{-1}). The Theil-Sen slopes of the grass pollen are actual 10 times higher (scaling applied).

the pollen season. Introducing time lags may reveal other correlations that could be helpful. For instance, from observations at Brussels we obtain a strong (negative) correlation (R = −0.76) between the summer precipitation (June, July, August) and the SPIn of birch for the next season for the period 2008–2019. Expanding the period back to 1982, deteriorates the relationship. The correlation between averaged summer air temperature and SPIn of the next season is +0.75, and if the summer precipitation and temperature ratio is used, then the correlation increases to +0.78. This suggests that the temperature and water stress might be a good indicator for estimating next season birch pollen SPIn. Something similar was found for the temperature and precipitation just before the start of the grass pollen season (Kurganskiy et al., 2021) or using the annual mean temperature of the previous year (Zhang and Steiner, 2022).

4. Conclusions and future research

The introduction of dynamic birch tree fraction maps for the period 1982–2019 intensifies the climate change induced increase of the amount of birch pollen in the air, but for some locations in Belgium it has a dampening effect. The rise in birch pollen amounts over time are associated with decreases in rainfall and the eastward horizontal wind component and an increase in radiation. However, when focusing on the contribution of birch pollen emission sources only, the overall

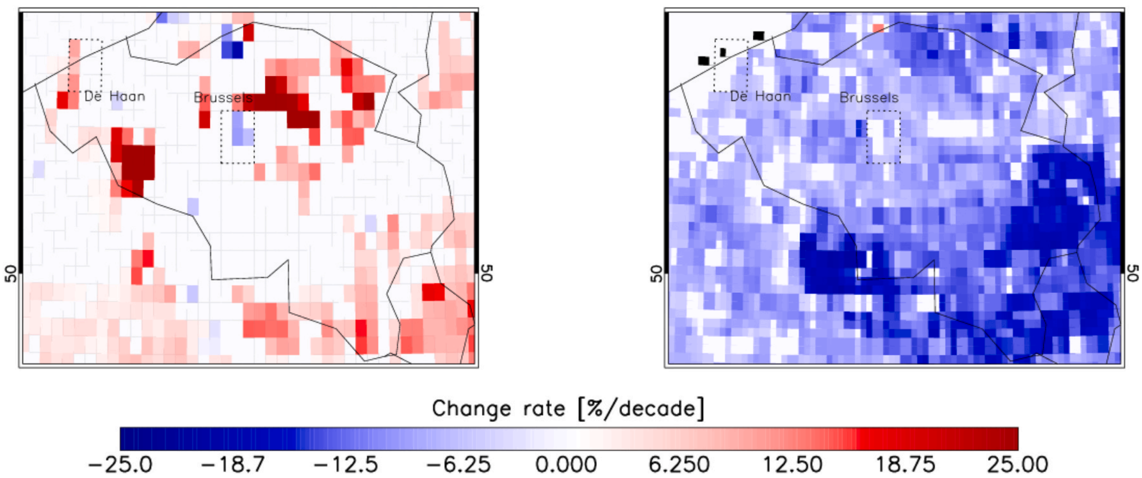

Fig. 10. Decadal change rate in Theil-Sen slopes of birch pollen emission sources (left panel, reprocessed from Verstraeten et al., 2022) and grass pollen emission sources (right panel) between 1982 and 2019 based on the Random Forest methodology and the NDVI time series.

associations between birch pollen concentrations and precipitation and wind are positive. Introducing dynamic grass pollen emission maps resulted in a decrease of grass pollen concentrations over time. The reduction is mainly positively associated with changes in precipitation and wind, and is negatively associated with for radiation.

Although SILAM is a well-established model, uncertainties associated with the pollen emission parameterizations (i.e. these values can change over time) might limit the model outcome. Increasing number of observations across space and time could improve our understanding of pollen production and help in better constraining model simulations. This study provides a tool for evaluating the past and future changes in climate and the possible consequences on pollen production and their corresponding health effects. Despite the limitation of this study, we could quantify how trends in airborne grass and birch pollen concentrations over almost four decades in Belgium are associated with climate change and with changes in the spatial distribution of the pollen production. Moreover, we show that the spatial variations of these associations might be substantial even on the scales of small countries.

Future research should focus on how well pollen transport models perform using highly detailed maps with pollen emission sources over a long time period as conducted in this study. More investigations are required on the impact of climate-induced changes in plant physiology and how they affect current model parametrizations. Furthered, the use of ECMWF ERA5 meteorology compared to ECMWF FORECAST data in pollen transport might lead to different outcomes. Moreover, also the meteorological conditions in the months preceding the actual pollen season have shown impact on pollen emissions. Assimilating these data can be helpful to refine the pollen transport model parameterization to increase the pollen forecasting skills of the upcoming pollen season.

Funding

This research was partly funded by the Belgian Science Policy Office (BELSPO) in the frame of the Belgian Research Action through Interdisciplinary Networks Brain (BRAIN.be) programme – project RETROPOLLEN (B2/191/P2/RETROPOLLEN) and partly funded by the Royal Meteorological Institute of Belgium. The SILAM general development has been funded by the Academy of Finland project PS4A (grant 318194).

CRediT authorship contribution statement

Willem W. Verstraeten: Conceptualization, Methodology, model, Software, Formal analysis, Investigation, Visualization, Project administration, Funding acquisition, Writing – original draft, preparation, Resources, Data curation, All authors have read and agreed to the published version of the manuscript. **Nicolas Bruffaerts:** Conceptualization, Methodology, Project administration, Funding acquisition, Resources, Data curation, Writing – review & editing, All authors have read and agreed to the published version of the manuscript. **Rostislav Kouznetsov:** model, Software, Resources, Writing – review & editing, All authors have read and agreed to the published version of the manuscript. **Letty de Weger:** Writing – review & editing, All authors have read and agreed to the published version of the manuscript. **Mikhail Sofiev:** model, Software, Resources, Writing – review & editing, All authors have read and agreed to the published version of the manuscript. **Andy W. Delcloo:** model, Software, Project administration, Funding acquisition, Resources, Data curation, Writing – review & editing, All authors have read and agreed to the published version of the manuscript.

Declaration of competing interest

The authors declare that they have no known competing financial interests or personal relationships that could have appeared to influence the work reported in this paper.

Data availability

Data will be made available on request.

References

Aerts, R., Bruffaerts, N., Somers, B., Demoury, C., Plusquin, M., Nawrot, T.S., Hendrickx, M., 2021. Tree pollen allergy risks and changes across scenarios in urban green spaces in Brussels, Belgium. Landsc. Urban Plann. 207, 104001, 2021.

Anderegg, W.R.L., Abatzoglou, J.T., Anderegg, L.D.L., Bielory, L., Kinney, P.L., Ziska, L., 2021. Anthropogenic climate change is worsening North American pollen seasons. Proc. Natl. Acad. Sci. USA 2021, 118. https://doi.org/10.1073/pnas.2013284118.

Bauchau, V., Durham, S.R., 2004. Prevalence and rate of diagnosis of allergic rhinitis in Europe. Eur. Respir. J. 24, 758–764. https://doi.org/10.1183/09031936.04.00013904, 2004.

Beggs, P.J., 2021. Climate change, aeroallergens, and the aeroexposome. Environ. Res. Lett. 16 (3), 035006 https://doi.org/10.1088/1748-9326/abda6f.

Blomme, K., Tomassen, P., Lapeere, H., et al., 2013. Prevalence of allergic sensitization versus allergic rhinitis symptoms in an unselected population. Int. Arch. Allergy Immunol. 160 (2), 200–207.

Bruffaerts, N., De Smedt, T., Delcloo, A., Simons, K., Hoebeke, L., et al., 2018. Comparative long-term trend analysis of daily weather conditions with daily pollen concentrations in Brussels, Belgium. Int. J. Biometeorol. 62 (3), 483–491. https://doi.org/10.1007/s00484-017-1457-3.

Charalampopoulos, A., Damialis, A., Lazarina, M., Halley, J.M., Vokou, D., 2021. Spatiotemporal assessment of airborne pollen in the urban environment: the pollenscape of Thessaloniki as a case study. Atmos. Environ. 247, 118185, 2021.

Damialis, A., Halley, J.M., Gioulekas, D., Vokou, D., 2007. Long-term trends in atmospheric pollen levels in the city of Thessaloniki, Greece. Atmos. Environ. 41, 7011–7021, 2007.

de Weger, L.A., Bruffaerts, N., Koenders, M.M.J.F., et al., 2021. Long-term pollen monitoring in the Benelux: evaluation of allergenic pollen levels and temporal variations of pollen seasons. Frontiers in Allergy 2 (30). https://doi.org/10.3389/falgy.2021.676176.

Delcloo, A., Verstraeten, W.W., Dujardin, S., et al., 2020. Spatio-temporal monitoring and modelling of birch pollen in Belgium. Air Pollution Modeling and its Application XXVI. https://doi.org/10.1007/978-3-030-22055-6_12.

Delcloo, A., Verstraeten, W.W., Kouznetsov, R., Bruffaerts, N., Dujardin, S., Hendrickx, M., Sofiev, M., 2021. Spatio-temporal modeling of grass and birch pollen in Belgium. In: Mensink, C., Matthias, V. (Eds.), Air Pollution Modeling and its Application XXVII. ITM 2019. Springer Proceedings in Complexity. Springer, Berlin, Heidelberg. https://doi.org/10.1007/978-3-662-63760-9_17.

D'Amato, G., Cecchi, L., Bonini, S., et al., 2007. Allergenic pollen and pollen allergy in Europe. Allergy 62, 976–990. https://doi.org/10.1111/j.1398-9995.2007.01393.x.

ECMWF. European Centre for Medium-Range Weather Forecasts. https://www.ecmwf.int/en/newsletter/147/news/era5-reanalysis-production.

ENDVI10, 2021. Normalized Difference Vegetation Index. PRODUCTS: LSA-420 AND LSA-454 (ENDVI10). SAF/LAND/VITO/PUM_ENDVI10v2Issue/Revision Index: Issue 3. Last Change: 21/01/2021. https://nextcloud.lsasvcs.ipma.pt/s/tmDP8S5HomDSPd4?dir=undefined&openfile=136004. (Accessed 10 March 2021).

Fu, Y.H., Zhao, H., Piao, S., Peaucelle, M., Peng, S., Zhou, G., Ciais, P., Huang, M., Menzel, A., Peñuelas, J., Song, Y., Vitasse, Y., Zeng, Z., Janssens, I.A., 2015. Declining global warming effects on the phenology of spring leaf unfolding. Nature 526, 104–107. https://doi.org/10.1038/nature15402.

Galán, C., Alcázar, P., Oteros, J., et al., 2016. Airborne pollen trends in the Iberian Peninsula. Sci. Total Environ. 550, 53–59, 2016.

García-Mozo, H., Yaezel, L., Oteros, J., Galán, C., 2014. Statistical approach to the analysis of olive long-term pollen season trends in southern Spain. Sci. Total Environ. 473–474, 103–109.

Hirst, J.M., 1952. An automatic volumetric Spore Trap. Ann. Appl. Biol. 39, 257–265. https://doi.org/10.1111/j.1744-7348.1952.tb00904.x.

Hoebeke, L., Bruffaerts, N., Verstraeten, C., Delcloo, A., Desmedt, T., et al., 2018. Thirty-four years of pollen monitoring: an evaluation of the temporal variation of pollen seasons in Belgium. Aerobiologia 34, 139. https://doi.org/10.1007/s10453-017-9503-5.

IPCC, 2022. Climate Change 2022: Impacts, Adaptation, and Vulnerability. Contribution of Working Group II to the Sixth Assessment Report of the Intergovernmental Panel on Climate Change (H. -O. Pörtner, D.C. Roberts, M).

Kouznetsov, R., Sofiev, M., 2012. A methodology for evaluation of vertical dispersion and dry deposition of atmospheric aerosols. J. Geophys. Res. 117 https://doi.org/10.1029/2011JD016366.

Kurganskiy, A., Creer, S., de Vere, N., et al., 2021. Predicting the severity of the grass pollen season and the effect of climate change in Northwest Europe. Sci. Adv. https://doi.org/10.1126/sciadv.abd76.

Langanke, T., 2017. Copernicus LandMonitoring Service – High Resolution Layer Grassland: Product Specifications Document. Copernicus team at EEA. https://land.copernicus.eu/user-corner/technical-library/hrl-grassland-technical-document-prod-2015. (Accessed 6 April 2020).

Lind, T., Ekebom, A., Alm Kübler, K., Östensson, P., Bellander, T., Lõhmus, M., 2016. Pollen season trends (1973-2013) in Stockholm area, Sweden. PLoS One 11 (11), e0166887. https://doi.org/10.1371/journal.pone.0166887.

Linkosalo, T., Ranta, H., Oksanen, A., Siljamo, P., Luomajoki, A., Kukkonen, J., et al., 2010. A double-threshold temperature sum model for predicting the flowering duration and relative intensity of Betula pendula and B. pubescens. Agric. For. Meteorol. 150, 6–11. https://doi.org/10.1016/j.agrformet.2010.08.007.

Makra, L., Matyasovszky, I., Deak, A.J., 2011. Trends in the characteristics of allergenic pollen circulation in central Europe based on the example of Szeged, Hungary. Atmos. Environ. 45, 6010–6018.

Maya-Manzano, J.M., Skjøth, C.A., Smith, M., Dowding, P., Sarda-Estève, R., Baisnée, D., McGillicuddy, E., Sewell, G., O'Connor, D.J., 2021. Spatial and temporal variations in the distribution of birch trees and airborne Betula pollen in Ireland. Agric. For. Meteorol. 298–299, 108298 https://doi.org/10.1016/j.agrformet.2020.108298.

Pinzon, J.E., Tucker, C.J., 2014. A non-stationary 1981–2012 AVHRR NDVI3g time series. Rem. Sens. 6, 6929–6960.

Sen, P.K., 1968. Estimates of the regression coefficient based on Kendall's tau. J. Am. Stat. Assoc. 63 (324), 1379–1389. https://doi.org/10.2307/2285891.

Sofiev, M., 2017. On impact of transport conditions on variability of the seasonal pollen index. Aerobiologia 33, 167–179. https://doi.org/10.1007/s10453-016-9459-x.

Sofiev, M., Siljamo, P., Ranta, H., Rantio-Lehtimäki, A., 2006. Towards numerical forecasting of long-range air transport of birch pollen: theoretical considerations and a feasibility study. Int. J. Biometeorol. 50, 392–402. https://doi.org/10.1007/s00484-006-0027-x.

Sofiev, M., Siljamo, P., Ranta, H., Linkosalo, T., Jaeger, S., Rasmussen, A., Rantio-Lehtimaki, A., Severova, E., Kukkonen, J., 2013. A numerical model of birch pollen emission and dispersion in the atmosphere. Description of the emission module. Int. J. Biometeorol. 57, 45–58. https://doi.org/10.1007/s00484-012-0532-z.

Sofiev, M., Berger, U., Prank, M., Vira, J., Arteta, J., Belmonte, J., et al., 2015. MACC regional multi-model ensemble simulations of birch pollen dispersion in Europe. Atmos. Chem. Phys. 15, 8115–8130, 2015.

Theil, H., 1950. A rank-invariant method of linear and polynomial regression analysis. I, II, III. Nederl. Akad. Wetensch., Proc. 53 (386–392), 1397–1412, 521–525.

To, T., Stanojevic, S., Moores, G., et al., 2012. Global asthma prevalence in adults: findings from the cross-sectional world health survey, 2012 BMC Publ. Health 12, 204. -204.

Tong, S., Beggs, P.J., Davies, J.M., et al., 2022. Compound impacts of climate change, urbanization and biodiversity loss on allergic disease. Int. J. Epidemiol. https://doi.org/10.1093/ije/dyac197/ dyac197.

Tucker, C.J., 1979. Red and photographic infrared linear combinations for monitoring vegetation. Remote Sens. Environ. 8, 127–150.

Velasco-Jiménez, M.J., Alcázar, P., Díaz de la Guardia, C., et al., 2020. Pollen season trends in winter flowering trees in South Spain. Aerobiologia 36, 213–224, 2020.

Vélez-Pereira, A.M., De Linares, C., Belmonte, J., 2022. Aerobiological modelling II: a review of long-range transport models. Sci. Total Environ. 845 https://doi.org/10.1016/j.scitotenv.2022.157351.

Verstraeten, W.W., Boersma, K.F., Douros, J., Williams, J.E., Eskes, H., Liu, F., Beirle, S., Delcloo, A., 2018. Top-down NOX emissions of European cities based on the downwind plume of modelled and space-borne tropospheric NO2 columns. Sensors 18, 2893. https://doi.org/10.3390/s18092893.

Verstraeten, W.W., Dujardin, S., Hoebeke, L., Bruffaerts, N., Kouznetsov, R., Dendoncker, N., Hamdi, R., Linard, C., Hendrickx, M., Sofiev, M., Delcloo, A.W., 2019. Spatio-temporal monitoring and modelling of birch pollen levels in Belgium. Aerobiologia 35 (4), 703–717. https://doi.org/10.1007/s10453-019-09607-w.

Verstraeten, W.W., Kouznetsov, R., Hoebeke, L., Bruffaerts, N., Sofiev, M., Delcloo, A.W., 2021. Modelling grass pollen levels in Belgium. Sci. Total Environ. 753, 141903 https://doi.org/10.1016/j.scitotenv.2020.141903.

Verstraeten, W.W., Kouznetsov, R., Hoebeke, L., Bruffaerts, N., Sofiev, M., Delcloo, A.W., 2022. Reconstructing multi-decadal airborne birch pollen levels based on NDVI data and a pollen transport model. Agric. For. Meteorol. 320 (2), 108942 https://doi.org/10.1016/j.agrformet.2022.108942.

WHO, 2003. Phenology and Human Health: Allergic Disorders. WHO, Copenhagen.

WMO, 2020. The State of the Global Climate 2020. https://public.wmo.int/en/ourmandate/climate/wmo-statement-state-of-global-climate.

Zhang, Y., Steiner, A.L., 2022. Projected climate-driven changes in pollen emission season length and magnitude over the continental United States. Nat. Commun. 13, 1234. https://doi.org/10.1038/s41467-022-28764-0.

Ziello, C., Sparks, T.H., Estrella, N., Belmonte, J., Bergmann, K.C., et al., 2012. Changes to airborne pollen counts across Europe. PLoS One 7 (4), e34076.

Ziska, L.H., 2021. Climate, carbon dioxide, and plant-based aero-allergens: a deeper botanical perspective. Frontiers in Allergy 2, 714724. https://doi.org/10.3389/falgy.2021.714724.

Ziska, L.H., Makra, L., Harry, S.K., et al., 2019. Temperature-related changes in airborne allergenic pollen abundance and seasonality across the northern hemisphere: a retrospective data analysis. Lancet Planet. Health 3 (3), e124–e131. https://doi.org/10.1016/S2542-5196(19)30015-4.